Mechanical Systems and Signal Processing (1994) 8(1), 1–19

MODELING AND IDENTIFICATION OF THE COMBUSTION PRESSURE PROCESS IN INTERNAL COMBUSTION ENGINES

FRANCIS T. CONNOLLY AND ANDREW E. YAGLE

Department of Electrical Engineering and Computer Science, 1301 *Beal Avenue, The University of Michigan, Ann Arbor, MI* 48109-2122, *U.S.A.*

(*Received* 15 *January* 1992, *accepted* 10 *September* 1992)

We present a new model relating cylinder combustion pressure to crankshaft angular velocity in an internal combustion engine. There are three aspects to this model. First, by changing the independent variable from time to crankshaft angle, a non-linear differential equation model becomes a linear first-order differential equation. Second, a new stochastic model for combustion pressure uses the sum of a deterministic waveform and a raised cosine window amplitude-modulated by a Bernoulli–Gaussian random sequence, parametrising the pressure by the sample modulating sequence. This results in a state equation for the square of angular velocity sampled every combustion, with the modulating sequence as input. Third, the inverse problem of reconstructing pressure from noisy angular velocity measurements can now be formulated as a state-space deconvolution problem, and solved using a Kalman-filter-based deconvolution algorithm. Simulation results show that the parametrised pressure can be deconvolved at low noise levels, and combustion misfires detected, all in real time. Supporting experimental results are referenced in companion papers.

1. INTRODUCTION

Automobile spark-ignited internal combustion (SI-IC) engines must satisfy increasingly stringent requirements on the reduction of exhaust gas emissions. This motivates more sophisticated analysis and modeling of IC engine operation and dynamics. One measure of the operation of an IC engine is the combustion pressure produced in the cylinders, since *cyclic variation* in combustion is a limitation of IC engine operation. This cycle-to-cycle variation becomes more significant as the air-to-fuel ratio becomes more efficient, i.e., is increased or leaned from the normal stoichiometric ratio used in present day SI-IC engines [1–7].

This motivates the work presented here, which has three major features: (1) reformulation of a non-linear differential equation relating the combustion pressure (P) to engine crankshaft angular velocity (denoted omega, Ω) into a linear first-order differential equation relating P to the square of the angular velocity Ω^2; (2) a new stochastic model for the combustion pressure P; and (3) application of signal processing system identification techniques to solve the inverse problem of determining the stochastic part of P from noisy observations of Ω. A limitation of our results so far is that they must be applied at steady-state operation (constant engine rotation speed and load torque).

The novelty of the work lies in the development of a new stochastic model of the combustion pressure P. P is modeled as a known deterministic waveform plus a stochastic part which is a Bernoulli–Gaussian sequence indexed by combustion number. Here

0888–3270/94/010019 + 19 $08.00/0

Bernoulli–Gaussian refers to a Gaussian-amplitude-modulated Bernoulli process. This allows stochastic deconvolution methods [8–10], which have been widely applied to seismic signal processing inverse problems, to be used to reconstruct P from observations of Ω. This is an improvement over previous methods, which attempt only a deterministic reconstruction of the P waveform while neglecting the stochastic nature of the combustion process, and for the most part neglect measurement noise [11–14]. It is the intent of the method presented in this paper to determine this stochastic part of combustion, in the form of estimation of a sequence parametrising cyclic combustion pressure variability. In the method proposed here, measurement noise is explicitly included in the inverse problem formulation.

Novel aspects of the work presented in the paper include: (1) using engine crankshaft angle (denoted θ) rather than time as the independent variable; (2) using a Bernoulli–Gaussian random sequence to model the stochastic part of combustion pressure P; (3) a recursive combustion-to-combustion model for the $P - \Omega$ relationship; and (4) application of signal processing and stochastic identification techniques to IC engine modeling, to reconstruct the combustion pressure P.

This paper is organized as follows: Section 2 states the problem and its relevance, and briefly reviews previous research in this area; Section 3 describes the new stochastic model of the combustion pressure P to angular velocity Ω relationship; Section 4 discusses methods for identification of the stochastic pressure sequence; Section 5 presents simulation results (experimental results are referenced in companion papers); and Section 6 concludes by summarising the results and discussing further work.

2. PROBLEM STATEMENT

The IC engine is a complex, non-linear mechanical system that is difficult to characterise completely over its wide operating region (usually given as a load torque or intake manifold pressure *vs* engine speed operating point plane). However, it is possible to characterise and model in a steady state condition a given specific subfunction or subsystem of engine operation.

2.1. INTRODUCTION

One such subfunction is the relationship between the combustions (and their resulting pressures) and the angular velocity of the engine, or more specifically, between the combustion variability and the small fluctuations of the angular velocity about its average (slowly-varying) value. The essence of the problem is that these fluctuations occur essentially on a combustion-to-combustion basis and contain information related to the combustion pressures that produced the torque which accelerates the crankshaft (other effects, such as the reciprocating motion of the piston assembly, can be accurately modeled). Figure 1 shows actual combustion pressure and angular velocity, respectively, both recorded simultaneously from an engine mounted in an automobile. Note the combustion-to-combustion cyclic variation in pressure (around the peak region), and the similar variation in the angular velocity waveform.

Our first goal is to model the relationship between the pressure fluctuations and the velocity fluctuations. If all the combustion pressures are the same, then the velocity variations will be periodic, while random fluctuations in velocity are caused in large part by the random pressure variation from combustion to combustion. Our first goal is to model the Ω resulting from a given combustion pressure P. Our second goal is then to solve the inverse problem of identifying P from Ω.

Engine models (at least for control and diagnostic purposes) generally fit into two categories: (1) models dealing with average behaviour over several or many engine cycles (such as present day control models); and (2) models dealing with more short-term behaviour, such as thermodynamic combustion models. The significance is that more effective engine operation and control may be achieved by modeling and controlling the engine on a combustion-to-combustion basis. The proposed model is of the second type, modeling the combustion-to-combustion fluctuations in Ω.

2.2. ENGINE TORQUES

The concepts underlying the engine model will now be explained. The model is based on a straightforward representation of the geometry of a single cylinder in an internal combustion (IC) engine, as shown in Fig. 2, and models for the individual torques acting on the crankshaft and piston. The geometry model reflects standard practice used in IC engine modeling [15, 16]; it depicts the cylinder walls, piston, crankshaft torque arm, connecting rod, and piston center axis line. Model parameters are listed in Table 1.

The torque applied to the crankshaft by the engine is composed of five major parts: (1) indicated torque $T_i(\theta)$; (2) reciprocating torque $T_r(\theta)$; (3) friction and pumping loss torque $T_{f_p}(\theta)$; (4) load torque $T_L(\theta)$; and (5) other less-significant fluctuating torques $T_0(\theta)$. The latter torques, $T_0(\theta)$, may be modeled as being insignificant compared to the first four terms [17].

$T_i(\theta)$ is due to the force generated by the combustion gas pressure $P(\theta)$. The equivalent mass of the piston assembly M_{eq} (mass of piston, wrist pin, piston rings, and the small end of the connecting rod) is subjected to accelerations during the engine cycle, due to its reciprocating motion, and as a result the reciprocating force $F_r(\theta)$ is generated along the direction of the piston axis. $F_r(\theta)$ produced no net energy in the system, but can cause significant fluctuations at the combustion frequency in the net torque $T_e(\theta)$ applied to the crankshaft. These fluctuations are approximately quadratically proportional to engine angular velocity. $T_r(\theta)$ is purely deterministic and completely described by engine geometry. $T_{fp}(\theta)$ represents energy loss due to friction and the pumping action

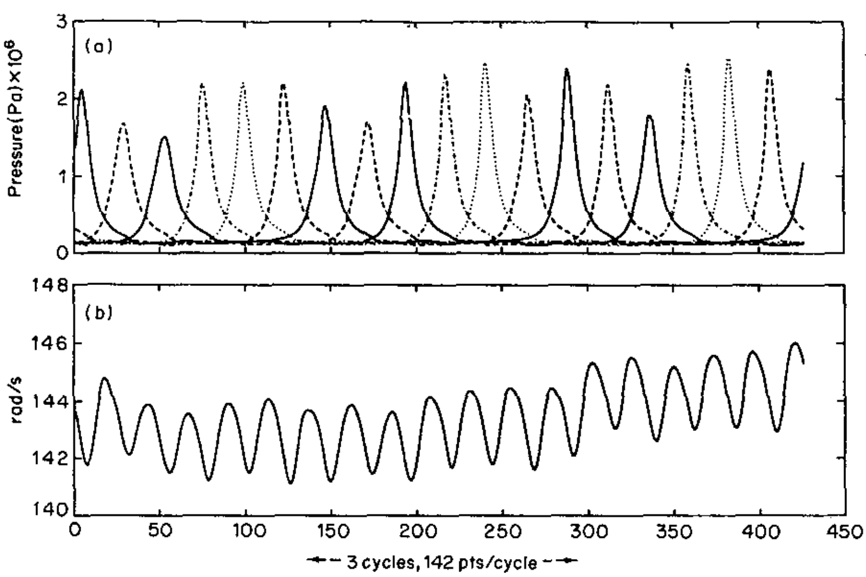

Figure 1. (a) Combustion pressure P and (b) corresponding angular velocity Ω measured from a six-cylinder engine for three engine cycles.

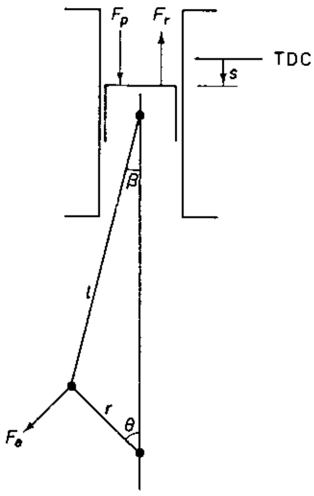

Figure 2. Cylinder geometry model.

(air/fuel/exhaust) of the engine. The instantaneous value of $F_{f_p}(\theta)$ during combustion proves to be difficult to measure, although the average value may be approximated via engine motoring tests (spinning of an engine without combustion, in a test stand or dynamometer) and its effect lumped in with $T_L(\theta)$. The fluctuating part of $F_{f_p}(\theta)$ is impulsive around the piston 'dead centres' (either end of the piston stroke) where the piston reverses direction, which is where the geometry function which transforms force in the piston axis direction to torque on the crank arm passes through zero.

The net result of these torques is expressed as

$$T_e(\theta) = T_i(\theta) + T_r(\theta) + T_{f_p}(\theta) + T_L(\theta) + T_0(\theta) \tag{1}$$

where $T_e(\theta)$ denotes the net torque acting on the engine. This equation reflects the effect

TABLE 1

Parameters used in the $P - \Omega$ IC engine model

s	piston displacement from TDC
r	crank radius
l	connecting rod length
A_p	piston face area
β	con rod angle from piston axis
θ	crank position angle
$\Omega(t) = \mathrm{d}\theta/\mathrm{d}t$	crankshaft angular velocity
M_{eq}	equivalent mass of reciprocating parts
$F_p(\theta)$	force due to combustion pressure
$F_r(\theta)$	force due to reciprocating mass
$F_e(\theta)$	net force applied to crankshaft torque arm
$F_{fp}(\theta)$	force due to friction and pumping
$T_e(\theta)$	rF_e, net torque applied to crankshaft
$T_i(\theta)$	indicated torque
$T_r(\theta)$	reciprocating torque
$T_{fp}(\theta)$	friction and pumping loss torque
$T_L(\theta)$	load torque
$T_0(\theta)$	other (less-significant) torques

of a single cylinder. The torque produced in a multi-cylinder engine can be described by summing an appropriate number of similar equations with correct cylinder phasing, assuming a stiff crankshaft. A model with a flexible crankshaft would include additional complexity to incorporate the flex between cylinders, yet the torque effect of each cylinder is essentially the same.

The above torque balance equation provides the basis for P-Ω models. The models differ in the degree of complexity the modeler is willing to impart to the physical configuration of the engine (e.g., flexible or stiff crankshaft, accessory and valve-train torques), the detail of the individual torque models, and the operating conditions under which the model is intended to reasonably reflect the engine dynamics.

2.3. PREVIOUS WORK

Several previous attempts have been made to reconstruct combustion pressure waveforms. The most common approach is estimation of the combustion pressure torque from measurements of the engine angular velocity, using an engine model such as the one in this paper [11, 12]. Another approach is measuring vibration acceleration at a point on the engine block (part of which is presumed to be caused by the combustions) and use of an appropriately identified transfer function or parametric model to compute the pressure waveform from a filtered vibration acceleration trace [13, 14]. A third approach involves using pattern recognition techniques on speed fluctuation waveforms [18].

Fehrenbach [11] uses a torque balance equation model, differing from that used in this paper by the addition of terms to include friction and valve train torque. The model uses only one cylinder and a stiff crankshaft is assumed. An inverse equation is derived by algebraically solving the torque balance equation for the combustion pressure, and then computing it through this inverse equation from filtered angular velocity measurements. One drawback of this method is the 'blank spots' in the pressure estimation at the cylinder's top dead centre (TDC) and bottom dead centre (BDC) during the engine cycle. This is due to the geometry function relating the combustion force to torque acting on the crank arm having value zero at top dead centre (TDC) and bottom dead centre (BDC). Since this function appears in the denominator of the inverse equation, no solution is possible at TDC and BDC.

Citron *et al.* [12] also use a model-based approach, with a more complex 4 dof model with an elastic crankshaft. They reconstruct the pressure using a method analogous to Fehrenbach's, utilising a portion of their inverse system, and are hence subject to the same 'dead spot' drawback. They also use θ as the independent variable, yet use Fourier series based on time as the inverse domain.

The second approach, used by Azzoni *et al.* [13, 14], employs measurements of engine block vibration acceleration and filtering to reconstruct the combustion pressure waveform. Cepstral filtering of the vibration acceleration (inspired by work in acoustics) is used to obtain a signal which is surmised to be highly correlated with the pressure signal, enabling estimation of the pressure signal via filtering. The filter is based on a transfer function model identified from measurements of the filtered vibration acceleration and combustion pressure.

The third approach by Brown and Neill [18] uses pattern recognition. A database of angular velocity waveforms is developed to which unknown waveforms may be matched to determine the corresponding peak combustion pressure.

The previous work discussed above all attempt to recover the continuous combustion pressure waveform(s), at least in the combustion region near the cylinder TDCs. None of the methods explicitly considers cyclic variability in their formulation. An advantage of the methods is that they are straightforward. However, their applicability is limited, since none of the methods appears to be implementable in real time. The methods do not have any stochastic features, and reduce measurement noise by low pass filtering.

This paper differs from the above work in that a stochastic model is used for part of the combustion pressure, and stochastic identification algorithms are used to derive a method for reconstructing the cyclic variation in the combustion pressure. Thus a stochastic characterisation of both the pressure process and the measurement noise is explicitly included in the model.

3. STOCHASTIC PRESSURE-ANGULAR VELOCITY MODEL

We first derive a model for the engine pressure to angular velocity relationship, starting from existing engine models [12, 15–17, 19, 20]. We start with a *torque balance equation* model, using well known engine modeling concepts. This is then developed into a differential equation model of the $P - \Omega$ relationship using crank angle θ as the independent variable. This model, in conjunction with a new stochastic combustion pressure model based on work in [20], is used to obtain a new recursive model indexed on a combustion-by-combustion basis. The recursive model is put into state-space form, permitting use of identification techniques such as Kalman-filter-based deconvolution algorithms to estimate the stochastic pressure process driving the recursive model.

3.1. ENGINE MODEL

The *torque balance equation* relating the torques in (1) to the angular acceleration of the crankshaft is

$$J\ddot{\theta} = T_i(\theta) + T_r(\theta) + T_L(\theta) \tag{2}$$

where crankshaft angle $\theta \triangleq \theta(t)$, $\ddot{\theta} = d^2\theta/dt^2$, and J is the effective moment of inertia of the engine. This equation incorporates the major torques produced by the engine accelerating the crankshaft. Assumptions are as follows: the crankshaft is infinitely stiff; the mean of $T_{fp}(\theta)$ is lumped in $T_L(\theta)$; fluctuations in $T_0(\theta)$ and $T_{fp}(\theta)$ are negligible compared to the first three terms [this is why $T_0(\theta)$ and $T_{fp}(\theta)$ are present in (1) but not (2)]; the engine is operating in a steady-state condition (constant 'average' engine speed over many engine cycles, constant $T_L(\theta)$, and fully warmed with spark timing and fuel mixture fixed); and J is the effective moment of inertia of the rotating parts of the engine at that operating point.

The first and last assumptions imply that the engine is treated with rigid body motion. A more accurate engine model would include crankshaft and drive-line (i.e. engine, transmission, axles and tyres) elasticity and damping. While this could increase modeling accuracy, it would also increase model complexity significantly. This would in turn make formulation of the pressure identification problem more difficult. For this reason the engine is modeled simply by a single lumped inertia.

The model derivation is for an even-firing, four-stroke, six-cylinder engine, although in general any engine configuration may be used. The new model is based on transforming (2) into the θ domain, so that θ becomes the independent variable instead of t, where $\theta = \theta(t)$. This transformation is desirable for two reasons: (1) IC engine data acquisition systems sample synchronously with engine position; and (2) the θ-domain, as opposed to the time domain, affords a convenient formulation of the problem into a first-order, linear θ-varying differential equation in $\Omega^2(\theta)$, the square of the angular velocity. It is this formulation that allows application of the identification algorithms discussed in Section 4

Detailed models of the torques [15, 16] are substituted into equation (2), which becomes

$$J\ddot{\theta} = \sum_{i=1}^{6} [P_i(\theta) f_1(\theta - \phi_i)] + \sum_{i=1}^{6} M_{eq} [\dot{\theta}^2 f_2(\theta - \phi_i) + \ddot{\theta} f_3(\theta - \phi_i)] + T_L(\theta) \tag{3}$$

where $\phi_i = (2\pi/3)(i-1)$, $P_i(\theta)$ is pressure in the ith cylinder, and M_{eq} is the mass of the reciprocating parts associated with each cylinder (assumed to be the same for all cylinders). The functions $f_1(\theta)$, $f_2(\theta)$, and $f_3(\theta)$ are derived from the geometry of the single-cylinder model shown in Fig. 2 and relate the forces produced in the engine to torque applied on the crankshaft. Define

$$f(\theta) = \sin\theta + \frac{r}{l}\sin\theta\cos\theta\sqrt{1 - \frac{r^2}{l^2}\sin^2\theta}. \tag{4}$$

Then

$$f_1(\theta) = rA_p f(\theta) \tag{5}$$

$$f_2(\theta) = -r^2\left[\cos\theta + \frac{r}{l}\cos 2\theta\right] f(\theta) \tag{6}$$

$$f_3(\theta) = -r^2\left[\sin\theta + \frac{r}{2l}\sin 2\theta\right] f(\theta). \tag{7}$$

The engine cycle is 4π radians, or two revolutions for a four-stroke engine, but $f_2(\theta)$ and $f_3(\theta)$ are periodic with period 2π radians, so (3) becomes

$$J\ddot{\theta} = \sum_{i=1}^{6} [P_i(\theta) f_1(\theta - \phi_i)] + 2M_{eq} \sum_{i=1}^{3} [\dot{\theta}^2 f_2(\theta - \phi_i) + \ddot{\theta} f_3(\theta - \phi_i)] + T_L(\theta). \tag{8}$$

The next step is to use the chain rule to find the relation between functions in the time domain and their values at the sample times in the θ domain. Define $\bar{\Omega}(\theta)$ as

$$\bar{\Omega}(\theta) \triangleq \bar{\Omega}(\theta(t)) \triangleq = \frac{d}{dt}\theta(t) = \dot{\theta}(t), \tag{9}$$

i.e. $\bar{\Omega}(\theta)$ is the same quantity as $\Omega(t)$ expressed in the θ domain. Then

$$\ddot{\theta}(t) = \frac{d}{dt}\Omega(t) = \frac{d}{dt}\bar{\Omega}(\theta(t)) = \frac{d\bar{\Omega}(\theta)}{d\theta}\frac{d\theta}{dt}\bigg|_{\theta=\theta(t)} = \frac{d\bar{\Omega}(\theta)}{d\theta}\bar{\Omega}(\theta) = \frac{1}{2}\frac{d}{d\theta}[\bar{\Omega}(\theta)]^2. \tag{10}$$

Now substitute for $\dot{\theta}(t)$ and $\ddot{\theta}(t)$ in (8). This gives

$$\frac{J}{2}\frac{d}{d\theta}[\bar{\Omega}(\theta)]^2 = \sum_{i=1}^{6} [P_i(\theta) f_1(\theta - \phi_i)]$$

$$+ 2M_{eq} \sum_{i=1}^{3} \left[[\bar{\Omega}(\theta)]^2 f_2(\theta - \phi_i) + \frac{1}{2}\frac{d}{d\theta}[\bar{\Omega}(\theta)]^2 f_3(\theta - \phi_i) \right] + T_L(\theta). \tag{11}$$

Defining

$$x(\theta) \triangleq [\bar{\Omega}(\theta)]^2 \tag{12}$$

and collecting terms, (11) becomes (in the θ domain)

$$\left[\frac{J}{2} - M_{\text{eq}} \sum_{i=1}^{3} f_3(\theta - \phi_i)\right] \frac{\mathrm{d}}{\mathrm{d}\theta} [x(\theta)] + \left[2M_{\text{eq}} \sum_{i=1}^{3} f_2(\theta - \phi_i)\right] x(\theta) = \sum_{i=1}^{6} [P_i(\theta) f_1(\theta - \phi_i)] + T_L(\theta). \quad (13)$$

Now define the following:

$$u_1(\theta) = \left[\frac{J}{2} - M_{\text{eq}} \sum_{i=1}^{3} f_3(\theta - \phi_i)\right] \quad (14)$$

$$u_2(\theta) = \sum_{i=1}^{6} [P_i(\theta) f_1(\theta - \phi_i)] + T_L(\theta) \quad (15)$$

$$u_3(\theta) = 2M_{\text{eq}} \sum_{i=1}^{3} f_2(\theta - \phi_i) \quad (16)$$

$$A(\theta) = \frac{u_3(\theta)}{u_1(\theta)} \quad (17)$$

$$B(\theta) = \frac{u_2(\theta)}{u_1(\theta)}. \quad (18)$$

Substituting (14)–(18) into (13) yields

$$\frac{\mathrm{d}}{\mathrm{d}\theta} [x(\theta)] - A(\theta) x(\theta) = B(\theta). \quad (19)$$

This is a first-order, linear, θ-varying differential equation which has a known function [see (14), (15) and (18)] of combustion pressure as the forcing function. The solution to (19) can be written in closed form as

$$x(\theta) = \mathrm{e}^{\int_0^\theta A(\mu)\,\mathrm{d}\mu} \int_0^\theta B(\alpha)\, \mathrm{e}^{-\int_0^\alpha A(\mu)\,\mathrm{d}\mu}\, \mathrm{d}\alpha + x(0)\, \mathrm{e}^{\int_0^\theta A(\mu)\,\mathrm{d}\mu} \quad (20)$$

Analysis of $A(\theta)$ and $u_1(\theta)$ show that they may be well approximated by trigonometric functions

$$A(\theta) \approx A_1 \sin(3\theta) \quad (21)$$

$$u_1(\theta) \approx c_1 + c_2 \cos(3\theta) \quad (22)$$

where $A_1 = -0{\cdot}018897$, $c_1 = 0{\cdot}040857$ and $c_2 = 2{\cdot}4938 \times 10^{-04}$ are constants. The sum of squared errors for one engine cycle (720 points/cycle) for these $A(\theta)$ and $u_1(\theta)$ approximations are, respectively, $3{\cdot}62 \times 10^{-07}$ and $2{\cdot}52 \times 10^{-11}$ using typical engine parameters. Using the approximations (21) and (22), define $g(\theta)$ and $\bar{g}(\theta)$ as

$$\mathrm{e}^{\int_0^\theta A(\mu)\,\mathrm{d}\mu} \approx \mathrm{e}^{\frac{A_1}{3}(\cos(3\theta) - 1)} \triangleq g(\theta); \quad \mathrm{e}^{-\int_0^\theta A(\mu)\,\mathrm{d}\mu} \approx \mathrm{e}^{-\frac{A_1}{3}(\cos(3\theta) - 1)} \triangleq \bar{g}(\theta) \quad (23)$$

so that an approximation of (20) is

$$x(\theta) = \bar{g}(\theta) \int_0^\theta B(\alpha) g(\alpha)\, \mathrm{d}\alpha + x(0) \bar{g}(\theta). \quad (24)$$

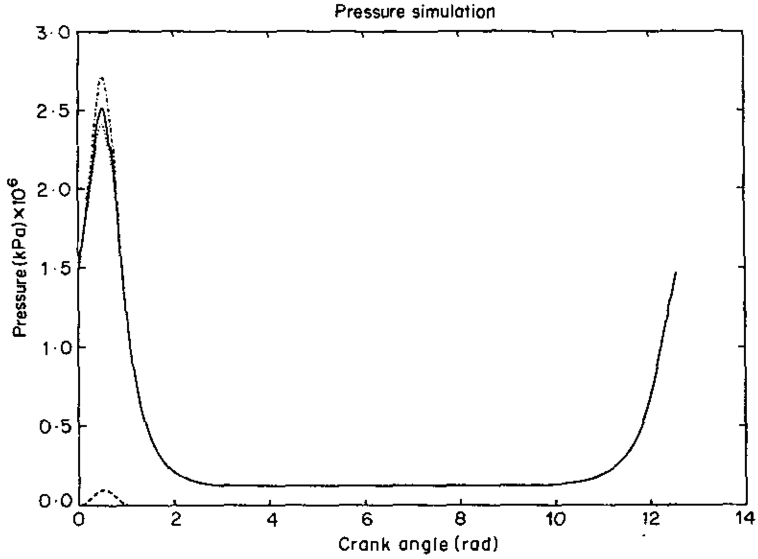

Figure 3. Stochastic pressure model and raised cosine for one cylinder, one engine cycle.

This approximation makes numerical computation of $x(\theta)$ tractable. Next we explain the stochastic P model, and then show how this model with (19) and (24) yield a recursive model for the stochastic $P - \Omega$ process.

3.2. STOCHASTIC PRESSURE MODEL

An analysis of the stochastic nature of the pressure process in an IC engine in a steady-state operating condition was carried out in [20], from a signal theoretic point of view. Several significant conclusions were made regarding the random nature of the combustion-to-combustion variation of the pressure process. First, the random variations in combustion (departure from mean pressure) occur in a *combustion variation region* starting at about TDC for the power stroke and extending for approximately 40 to 60° of engine revolution. Second, define the sequence of random variables $\xi_{\theta_0}(n)$ as the combustion pressure sampled as crank angle θ_0 in the nth engine cycle, where θ_0 is a fixed crank angle in the *combustion variation region.* Then the random sequence $\xi_{\theta_0}(n)$ is uncorrelated in n, wide sense stationary in n, and closely approximated as Gaussian with mean $\bar{P}_{\theta_0} = E\{P(\theta_0)\}$. Third, define the vector random process $\xi(n) = [\xi_{\theta_1}(n), \ldots, \xi_{\theta_N}(n)]^T$ as a vector of samples of cylinder pressure in the nth engine cycle at N different fixed crank angles $\theta_1, \ldots, \theta_N$ in the *combustion variation region.* Then the vector random sequence $\xi(n)$ is wide sense stationary in n, and well approximated by a jointly Gaussian vector random process.

We infer from these conclusions that the pressure process may be modeled as the sum of a deterministic mean pressure waveform and a Gaussian process correlated within the region of a particular combustion, but uncorrelated between combustions. Although this does not follow directly from [20], it seems reasonable in light of the conclusions in [20]. There is evidence to suggest that in *certain* engine operating conditions (e.g. for lean air-to-fuel ratios) there is correlation among combustions [21], but for the purposes of this paper the stochastic nature of combustion is *modeled* as an uncorrelated process.

A new signal-theoretic stochastic model for combustion pressure is proposed. We model the combustion pressure as the sum of a mean pressure waveform and a raised cosine waveform amplitude-modulated by a white Bernoulli–Gaussian random sequence indexed by combustion number. This sequence aggregates the effects of all cylinders into a compact, efficient parametrisation of combustion pressure. This parametrisation is pleasing as the deterministic, Newtonian relationship between combustion pressure and torque suggests that cyclic variability may be characterised by a single scalar value per combustion. The raised cosine window models deviation of instantaneous pressure from the mean pressure waveform, and has support (is non-zero) only during the *combustion variation region*. This window was chosen because it visually resembles real, observed pressure deviations, and also because of its simplicity in analysis and computation.

For a single cylinder, we model combustion pressure $P(\theta)$ as

$$P(\theta) = \bar{P}(\theta) + \xi(\theta) \tag{25}$$

where $\bar{P}(\theta)$ is the mean pressure waveform and the stochastic part of combustion is

$$\xi(\theta) = \begin{cases} \xi_n \frac{1}{2}[1 - \cos(6\theta)], & [\gamma_n, \gamma_n + \gamma_{\text{comb}}) \\ 0 & [\gamma_n + \gamma_{\text{comb}}, \gamma_{n+1}) \end{cases} \tag{26}$$

where ξ_n is a Bernoulli–Gaussian random sequence with Bernoulli probability of success $p = 1$ and Gaussian amplitude $\mathcal{N}(0, \sigma^2)$, n is the combustion-to-combustion index, $\gamma_n = n4\pi/N$ is the starting crankshaft angle of the nth combustion, $\gamma_{\text{comb}} = 4\pi/N$ is the angular duration of the combustion event, and N is the number of cylinders. The parametrising sequence is chosen as Bernoulli–Guassian to emphasise the 'spiky' nature of the sequence, as we are combining a continuous and a discrete model.

Figure 3 exhibits a typical realisation of stochastic pressure for the model devised for a single cylinder. The amplitude-modulated raised-cosine window added to the mean pressure waveform during the combustion region is depicted as a dashed line; the mean waveform $\bar{P}(\theta)$ is the solid line, and the two other lines depict typical realisations of the stochastic pressure model.

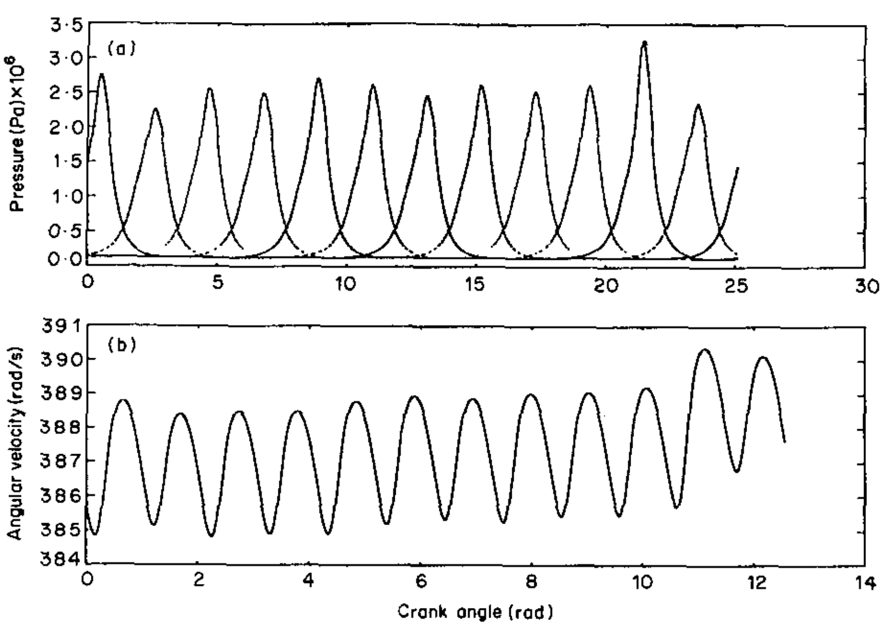

Figure 4. Typical forward simulation results (a) input pressure waveforms; (b) output angular velocity.

3.3. PRESSURE TO ANGULAR VELOCITY RECURSIVE MODELS

The closed-form solution approximation (24) is now used to develop a recursive $P - \Omega$ model. For a four-stroke even-firing six-cylinder engine, combustions occur every $4\pi/6$ radians of engine rotation. Let $\gamma_n = n(2\pi)/3$, $n = 0, 1, 2, \ldots$, and then set $\theta = \gamma_n$ and $\theta = \gamma_{n+1}$ in (24). This gives

$$x(\gamma_n) = \bar{g}(\gamma_n) \int_0^{\gamma_n} B(\alpha)g(\alpha)\,\mathrm{d}\alpha + x(0)\bar{g}(\gamma_n) \tag{27}$$

$$x(\gamma_{n+1}) = \bar{g}(\gamma_{n+1}) \int_0^{\gamma_{n+1}} B(\alpha)g(\alpha)\,\mathrm{d}\alpha + x(0)\bar{g}(\gamma_{n+1}) \tag{28}$$

and since $g(\gamma_{n+1}) = g(\gamma_n)$ [see equation (23)] we have

$$x(\gamma_{n+1}) - x(\gamma_n) = \bar{g}(\gamma_n) \int_{\gamma_n}^{\gamma_{n+1}} B(\alpha)g(\alpha)\,\mathrm{d}\alpha. \tag{29}$$

Equations (15), (18), (22) and (25) may be combined into

$$B(\theta) \approx \frac{1}{c_1 + c_2\cos(3\theta)} \left\{ \sum_{i=1}^{6} [(\bar{P}_i(\theta) + \xi_i(\theta))f_1(\theta - \phi_i)] + T_L(\theta) \right\} \tag{30}$$

where $\phi_i = (2\pi/3)(i-1)$ and i indicates cylinder number. Then

$$\int_{\gamma_n}^{\gamma_{n+1}} B(\theta)g(\theta)\,\mathrm{d}\theta = \int_{\gamma_n}^{\gamma_{n+1}} \frac{g(\theta)}{c_1 + c_2\cos(3\theta)} \left(\sum_{i=1}^{6} [\bar{P}_i(\theta)f_1(\theta - \phi_i)] + T_L(\theta) \right) \mathrm{d}\theta + \int_{\gamma_n}^{\gamma_{n+1}} \frac{g(\theta)}{c_1 + c_2\cos(3\theta)} \sum_{i=1}^{6} \xi_i(\theta)f_1(\theta - \phi_i)\,\mathrm{d}\theta. \tag{31}$$

The integral of $B(\theta)g(\theta)$ can thus be seen to have two parts: a deterministic part [the first term on the right-hand side of equation (31)], and a stochastic part (the second term on

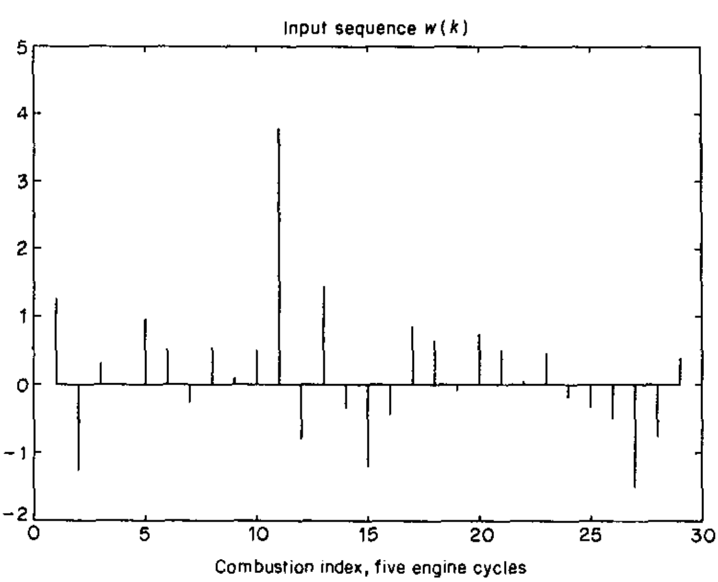

Figure 5. Input sequence used in simulation.

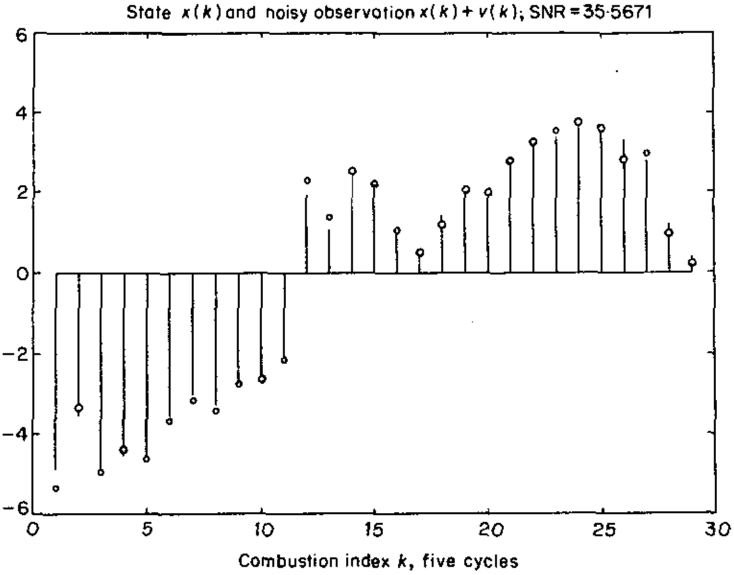

Figure 6. State $x(k)$ (——) and noisy observation $x(k)+v(k)$ (○).

the right-hand side). Since by assumption the engine is operating in a steady-state condition [constant $T_L(\theta) = T_L$ and average speed], the mean part of the deterministic indicated torque [the sum involving $\bar{P}_i(\theta)$] is opposed and cancelled by the constant load torque T_L. The deterministic part of the integral was numerically evaluated for this case using the mean pressure waveform simulation shown in Fig. 3. This deterministic part is

$$\bar{B}_n \triangleq \bar{g}(\gamma_n) \int_{\gamma_n}^{\gamma_{n+1}} \frac{1}{c_1 + c_2 \cos(3\theta)} \left\{ \sum_{i=1}^{6} [\bar{P}_i(\theta) f_i(\theta - \phi_i)] + T_L(\theta) \right\} d\theta. \qquad (32)$$

In steady-state $\bar{B}_n = \bar{B}$ evaluates to zero.

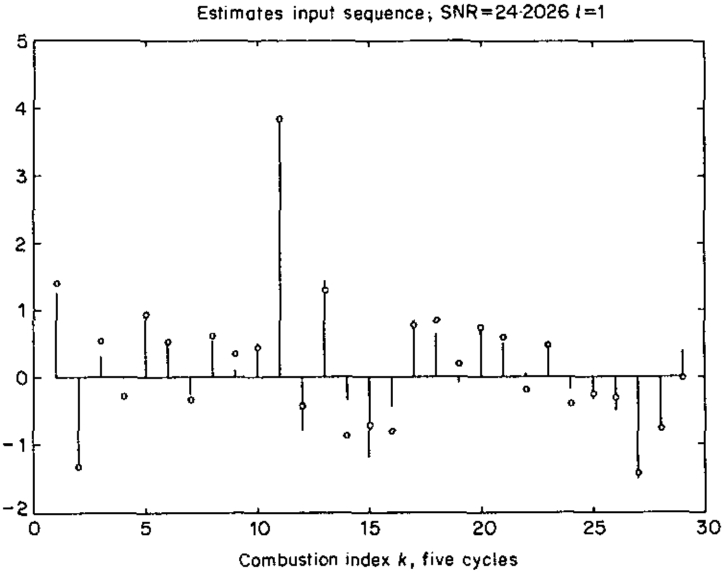

Figure 7. Output of optimal smoother, $\hat{w}(k|k+1)$, (○) compared with $w(k)$ (——).

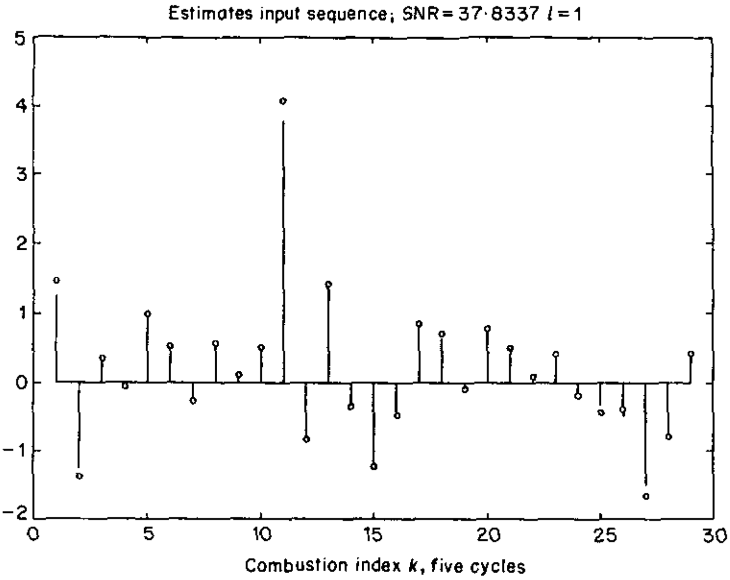

Figure 8. Output of optimal smoother, $\hat{w}(k|k+1)$, (○) compared with $w(k)$ (——).

In the stochastic part of the integral, it should be noticed that the raised cosines weighted by the Bernoulli–Gaussian sequence are independent from combustion to combustion. This means that for an integration over a combustion starting at a particular γ_n

$$\sum_{i=1}^{6} \xi_i(\theta) f_1(\theta - \phi_i) = \xi_m(\theta) f_1(\theta - \phi_m) = \xi_n \tfrac{1}{2}[1 - \cos(6(\theta - \phi_m))] f_1(\theta - \phi_m) \qquad (33)$$

where $\phi_m = (2\pi/3)(m-1)$, $m = (n \bmod 6) + 1$ is the index of the cylinder firing at γ_n, and n is the combustion index. This relation holds only where the raised cosine has support,

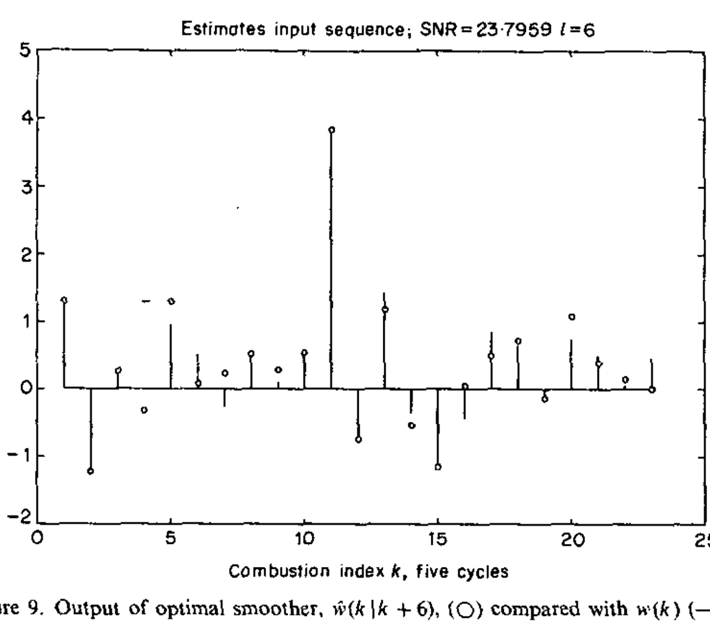

Figure 9. Output of optimal smoother, $\hat{w}(k|k+6)$, (○) compared with $w(k)$ (——).

that is, in the combustion region for that combustion [(see equation (26)]; the quantity on the far left of equation (33) is thus zero outside this region. Thus the stochastic part of the integral is a constant $\bar{b}$ weighted by the combustion-to-combustion random sequence ξ_n:

$$\xi_n \bar{b} = \xi_n \bar{g}(\gamma_n) \int_{\gamma_n}^{\gamma_{n+1}} \frac{g(\theta)}{c_1 + c_2 \cos(3\theta)} \frac{1}{2} [1 - \cos(6(\theta - \phi_m))] f_1(\theta - \phi_m) \, d\theta. \tag{34}$$

Note that $\bar{b}$ is independent of n, since the integrand above and $\bar{g}(\theta)$ are periodic in the combustion interval. The quantity $\bar{b}$ was numerically computed and found to be 0·0024205. Then

$$\int_{\gamma_n}^{\gamma_{n+1}} B(\alpha) g(\alpha) \, d\alpha = \bar{B}_n + \bar{b}\xi_n \tag{35}$$

and substituting $\bar{B}_n (= \bar{B} = 0$ at steady state), $\bar{b}$, and replacing $n \to \gamma_n$ in (29) yields

$$x(n+1) = x(n) + \bar{b}\xi_n \tag{36}$$

which is the discrete recursive formulation of the $P - \Omega$ process, in terms of squared angular velocity $x(n)$ [see equation (12)] as a function of combustion index n.

4. IDENTIFICATION

Three different methods were evaluated for estimating the combustion pressure from angular velocity measurements. The methods are briefly reviewed in this section, and simulation results presented in the next.

The first method was adaptive recursive least squares (RLS). Equation (3) was manipulated so that the unknown parameters, including the combustion pressures $P_i(\theta)$, appear in a linear regression, whose parameters are time varying. In this way simultaneous

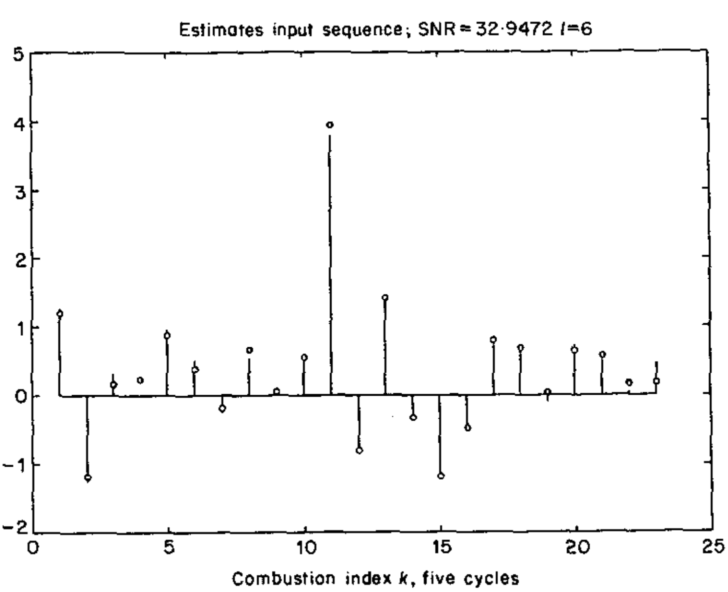

Figure 10. Output of optimal smoother, $\hat{w}(k|k+6)$, (○) compared with $w(k)$ (——).

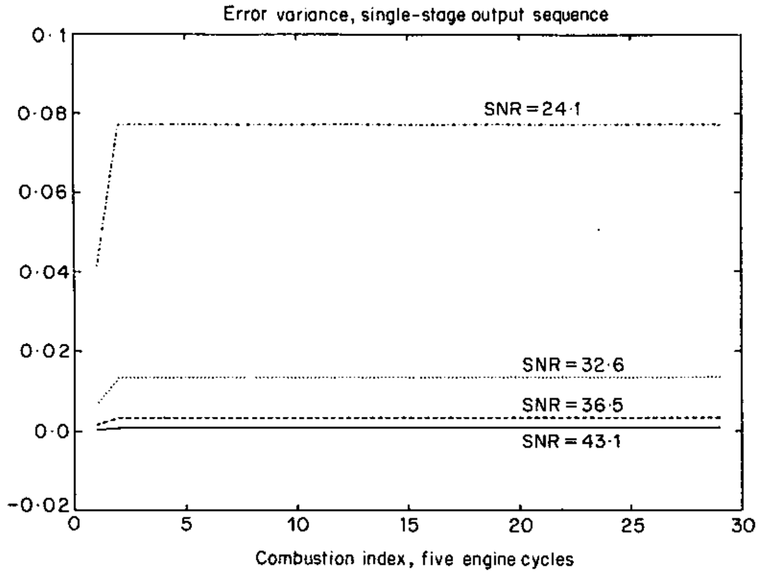

Figure 11. Error variance $\sigma^2_{\hat{w}}(k|k+1)$ vs combustion index.

recovery of the complete combustion pressure waveform for each cylinder was attempted. Several variations of adaptive RLS all proved unstable, as indicated by failure of the regressors to meet the persistent excitation condition for RLS. Consequently this method was abandoned.

The second method was Kalman-filter-based deconvolution. Equation (36) may be combined with an equation of noisy observations to give

$$x(n+1) = x(n) + \bar{b}w(n); \quad y(n) = x(n) + v(n) \tag{37}$$

where $x(n)$ is the square of angular velocity [see equations (12) and (27)], $\bar{b}$ is defined by equation (34), $w(n) = \xi_n$ is the Bernoulli–Gaussian white driving sequence [which specifies the stochastic cyclic combustion variability—see equation (26)], and $y(n)$ is the noisy observation of the square of the angular velocity.

The formulation in equation (37) may be used in deconvolution methods [8] for optimal estimation of the driving sequence $w(n)$. In general, consider the multi-variable system

$$x(n+1) = \Phi(n)x(n) + \Gamma(n)w(n); \quad y(n) = H(n)x(n) + v(n) \tag{38}$$

where $x \in R^n$, $y \in R^m$, $w \in R^q$, $v \in R^m$; Φ, Γ, and H are of proper dimension; and $w(n)$ and $v(n)$ are uncorrelated zero mean random sequences for which

$$E\{w(n)w^T(l)\} = Q(n)\delta_{nl} \tag{39}$$

$$E\{v(n)v^T(l)\} = R(n)\delta_{nl}. \tag{40}$$

Note that w and v may be non-stationary. The single-stage optimal estimate $\hat{w}(n|n+1)$ of $w(n)$ and error covariance $\Psi_{\hat{w}}(n|n+1)$ of $\hat{w}(n|n+1)$ can be computed using [8]

$$\hat{w}(n|n+1) = Q\Gamma^T P^{-1}(n+1|n)K(n+1)\tilde{y}(n+1|n) \tag{41}$$

$$\Psi_{\hat{w}}(n|n+1) = Q - Q\Gamma^T H^T[HP(n+1|n)H^T + R]^{-1}H\Gamma Q \tag{42}$$

where the following Kalman filter equations are used:

$$\hat{x}(n+1|n) = \Phi\hat{x}(n|n) \tag{43}$$

$$P(n+1|n) = \Phi P(n|n)\Phi^T + \Gamma Q\Gamma^T \tag{44}$$

$$K(n+1) = P(n+1|n)H^T[HP(n+1|n)H^T + R]^{-1} \tag{45}$$

$$\tilde{y}(n+1|n) = y(n+1) - H\hat{x}(n+1|n) \tag{46}$$

$$\hat{x}(n+1|n+1) = \hat{x}(n+1|n) + K(n+1)\tilde{y}(n+1|n) \tag{47}$$

$$P(n+1|n+1) = [I - K(n+1)H]P(n+1|n). \tag{48}$$

Equations (38)–(48) may be applied directly to the present problem by setting $\Phi(n) = 1$, $\Gamma(n) = \bar{b}$, $H(n) = 1$, $w(n) = \xi_n$, $v(n)$ as the observation noise, and n as the combustion index. The l-stage estimate $\hat{w}(n|n+l)$ and its error covariance $\Psi_{\hat{w}}(n|n+l)$ may also be computed.

The third method was adaptive deconvolution. In [9] an adaptive estimation algorithm was coupled to a deconvolution algorithm. Lainiotis *et al.* demonstrated the ability of adaptive deconvolution to handle situations of model uncertainty. The method was investigated, but not simulated for the present problem, and is mentioned further in Section 6.

5. SIMULATION RESULTS

This section presents simulation results for the forward continuous stochastic $P - \Omega$ engine model, and for deconvolution of the white sequence driving the pressure process in the model. Figure 4 shows typical forward simulation waveforms for two engine cycles.

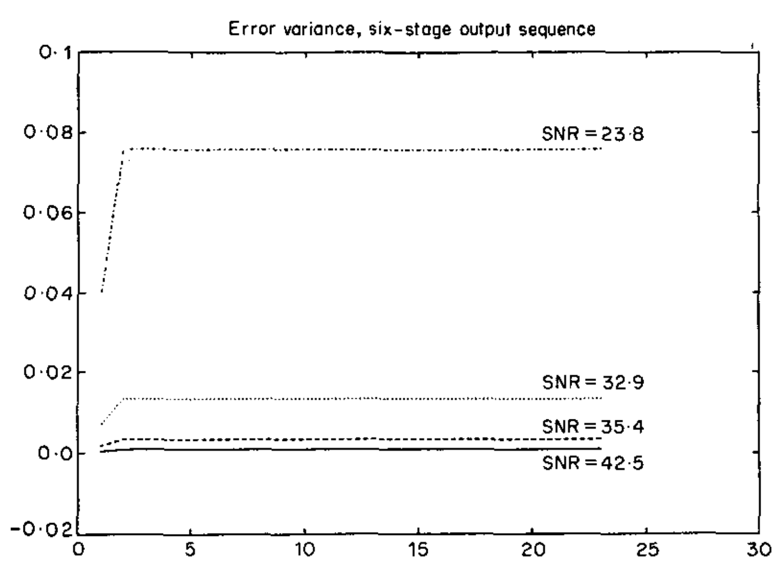

Figure 12. Error variance $\sigma^2_{\hat{w}}(k|k+6)$ vs combustion index.

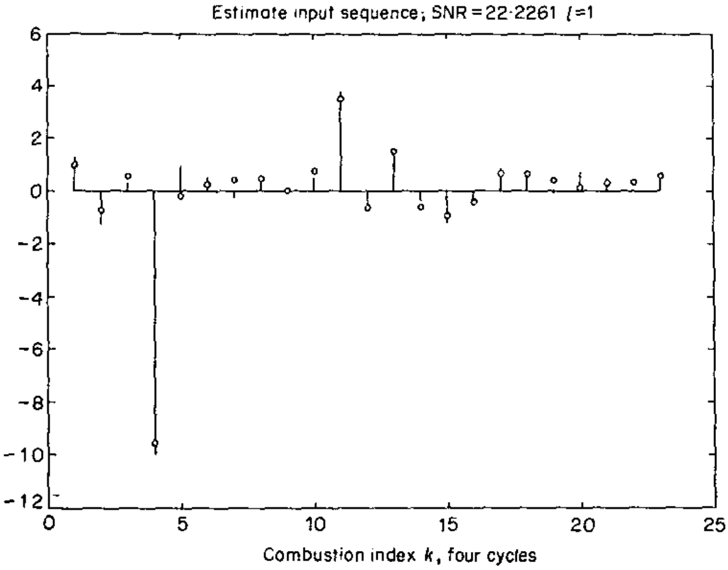

Figure 13. Output of optimal smoother, $\hat{w}(k \mid k+1)$, (○) compared with $w(k)$ (——) with one misfiring cylinder.

The upper plot shows six pressure waveforms used as the driving functions in the forward continuous simulation of equation (19). Note the variation in peak combustion pressure caused by the Bernoulli–Gaussian input sequence ξ_n. The corresponding output angular velocity waveform is shown on the lower plot. Note the variation in the speed fluctuations resulting from the variation in peak combustion pressure. Forward simulation waveforms exhibit visual qualitative behaviour very similar to that of typical observed engine speed waveforms. For example, compare the simulated speed waveform on Fig. 4 to the measured speed waveform on Fig. 1.

The goal is to estimate the combustion pressure variation from noisy measurements of angular velocity. The parametrised inverse problem is to estimate the Bernoulli–Gaussian white sequence ξ_n modulating the raised cosine window in the stochastic pressure model, from one sample of angular velocity from each combustion interval ($2\pi/3$ rad of crankshaft rotation). Figure 5 shows the input sequence used in the simulation; variations in the peak combustion pressures depicted in Fig. 4 correspond to variations in this input sequence. Figure 6 depicts the state $x(k)$ and noisy observations $y(k) = x(k) + v(k)$ for a typical signal-to-noise ratio (SNR). The SNR is computed as

$$\mathrm{SNR} = 10 \log \frac{\sum_{i=0}^{N-1} x^2(i)}{\sum_{i=0}^{N-1} v^2(i)} \tag{49}$$

where the sums are taken over the actual sample values used in a length N simulation.

Results are shown in Figs 7 to 10, which depict deconvolutions of the white sequence as outputs of the single- and l-stage optimal smoothers of [8] for several different conditions. Figure 11 shows the error variance $\phi_{\tilde{w}(n|n+1)}(k)$ and Fig. 12 shows the error variance $\phi_{\tilde{w}(k|k+6)}(k)$ for various SNRs. The results demonstrate that for low to moderate noise levels the optimal smoother performs a reasonably good deconvolution of the white sequence driving the stochastic combustion variability. The six-stage smoother appears to only give a moderate improvement over the one-stage smoother.

There is considerable interest in on-line detection of misfiring cylinders in automobile engines, especially in light of the proposed requirement [22] of an on-board diagnostic system capable of detecting a misfire rate above some predetermined threshold. The work presented here may be applicable to detection of misfires. Figure 13 shows a deconvolution wherein a misfiring cylinder is simulated by replacing one point in the driving Bernoulli–Gaussian sequence ξ_n with a large negative outlier, the effect of which is to significantly reduce the pressure in one cylinder during the corresponding combustion region (around the peak pressure). For the SNR shown, the deconvolution is able to detect this outlier, indicating that the method may be useful for detection of misfire.

Although only simulation results are shown in this paper, supporting experimental results may be found in [23, 25]. These experimental results indicate that the stochastic deconvolution is able to reasonably identify cyclic combustion pressure variation from real engine data, including the case of a misfiring cylinder.

6. CONCLUSION

A non-linear differential equation model of the combustion pressure to angular velocity relationship in an internal combustion engine was manipulated into a linear, first-order, θ-varying differential equation model (θ, the crankshaft angle, becomes the independent variable). This differential equation model was used to derive a novel discrete crank-angle recursion relating samples of engine angular velocity every combustion interval to a white Bernoulli–Gaussian sequence, which is a new model for cyclic combustion variability inherent in the combustion process. The recursion permits a state-space formulation with the white cyclic variability sequence as the input, to which stochastic state-space deconvolution methods for estimation of the input sequence may be applied. Simulations indicate that for low to moderate noise levels a reasonable deconvolution may be achieved. Experimental results supporting the theoretical developments are referenced in companion papers. These results indicate the feasibility and promise of measuring cyclic combustion pressure variability on-line using the deconvolution method, as the deconvolution estimator is scalar and simple to implement.

Topics for further study arise: (1) the use of multiple angular velocity observations per combustion (only one observation per combustion is utilised in the method developed in this paper); (2) combination of the stochastic deconvolution with a model adaptive procedure, forming an adaptive deconvolution [9]; (3) study of the application of the deconvolution method to the detection of combustion misfires (see Section 5); and (4) study of the random nature of the combustion pressure process, to the end of developing a more accurate stochastic cyclic combustion pressure model.

ACKNOWLEDGEMENT

This work was supported by the National Science Foundation under grant # MIP-8858082.

REFERENCES

1. D. J. PATTERSON 1966 *Technical Report* 660129, *SAE*. Cylinder pressure variations, a fundamental problem.
2. H. YAMAMOTO and M. MISUMI 1987 *Technical Report* 87054, *SAE*. Analysis of cyclic combustion variability in a lean operation SI engine.
3. Y. AL-ALOUSI and G. KARIM 1984 *Technical Report* 840232, *SAE*. Some considerations of cyclic variations in spark ignited engines fueled with gaseous fuels.

4. F. MATEKUNAS 1983 *Technical Report* 830337, *SAE*. Modes and measures of cyclic combustion variability.
5. M. BELMONT, M. HANCOCK and D. BUCKINGHAM 1986 *Technical Report* 860324, *SAE*. Statistical aspects of cyclic variability.
6. J. JANULA 1983 *International Journal of Vehicle Design* **4**, 587–604. The effect of cyclic dispersion of combustion pressure on working parameters of a spark ignited engine.
7. H. NOHIRA, T. KONOMI and S. ISHIYAMA 1980 *International Journal of Vehicle Design* **1**, 131–142. Analysis of cycle-by-cycle variation of combustion from pressure indicator data.
8. J. M. MENDEL 1977 *IEEE Transactions on Automatic Control* **22**, 694–706. White noise estimators for seismic data processing in oil exploration.
9. D. G. LAINIOTIS, S. K. KATSIKAS and S. D. LIKOTHANASIS 1988 *IEEE Transactions on Acoustics, Speech, and Signal Processing* **36**, 1715–1734. Adaptive deconvolution of seismic signals—Performance, computational analysis, parallelism.
10. D. G. LAINIOTIS, S. K. KATSIKAS and S. D. LIKOTHANASIS 1986 *Proceedings of Identification and Pattern Recognition Conference, Toulouse, France*, pp. 163–182. Minimum variance deconvolution.
11. H. FEHRENBACH 1990 *Proceedings 22nd International Symposium on Automotive Technology and Automation, Florence, Italy*, pp. 639–648. Model-based combustion pressure computation through crankshaft angular acceleration analysis.
12. S. CITRON, J. O'HIGGINS and L. CHEN 1984 *Technical Report* 890486, *SAE*. Cylinder by cylinder engine pressure and pressure torque waveform determination utilizing speed fluctuations.
13. P. AZZONI, G. CANTONI, G. MINELLI and E. PADOVANI 1990 *Proceedings 22nd International Symposium on Automotive Technology and Automation, Florence, Italy*. Combustion pressure recovering in spark ignition car engine.
14. P. AZZONI and A. PANIERO 1990 *Proceedings 22nd International Symposium on Automotive Technology and Automation, Florence, Italy*. Cylinder pressure reconstruction by cepstrum analysis.
15. L. LICHTY 1967 *Combustion Engine Processes*. New York: McGraw Hill.
16. E. OBERT 1964 *Internal Combustion Engines*. Scranton, PA: International Textbook Company.
17. K. IIDA, K. AKISHINO and K. KIDO 1990 *Technical Report* 900617, *SAE*. IMEP estimation from instantaneous crankshaft torque variation.
18. T. S. BROWN and W. S. NEILL *Technical Report* 920463, *SAE*. Determination of engine cylinder pressures from crank-shaft speed fluctuations.
19. S. REZEKA and N. HENEIN, 1984 *Technical Report* 840179, *SAE*. A new approach to evaluate instantaneous friction and its components in internal combustion engines.
20. G. RIZZONI 1986 *PhD Thesis, University of Michigan*. A dynamic model for the internal combustion engine.
21. J. K. MARTIN, S. L. PLEE and D. J. REMBOSKI 1988 *Technical Report* 880201, *SAE*. Burn modes and prior-cycle effects on cyclic variations in lean-burn spark-ignition engine combustion.
22. State of California Air Resources Board, May 5 1989. Mail-out #89-19. Malfunction and diagnostic system requirements applicable to new California passenger cars, light duty trucks, and medium duty vehicles with feedback fuel systems.
23. F. T. CONNOLLY 1992 *PhD Thesis, University of Michigan*. Modeling and identification of the combustion pressure process in internal combustion engines.
24. F. T. CONNOLLY and A. E. YAGLE 1993 *ASME Journal of Dynamic Systems, Measurement and Control*. In press. Modeling and identification of the combustion pressure process in internal combustion engines: experimental results.
25. F. T. CONNOLLY and A. E. YAGLE 1992 *Proceedings* 1992 *ASME Symposium on Advanced Transportation Technologies, Anaheim, Ca, November* 9–13. Modeling and identification of the combustion pressure process in internal combustion engines.